

# Optimal Gait Pattern Generation for Powered Robotic Exoskeleton and Verification of its Feasibility

Seunghoon Lee, Wansoo Kim, Minsung Kang, Jungsoo Han, Changsoo Han

**Abstract**— The will of humans with physical disabilities to move has found realization through the development of powered robotic exoskeleton. In this study, an energy-efficient gait pattern and swing trajectory of the powered robotic exoskeleton was proposed through function distribution analysis and the dynamic-manipulability ellipsoid (DME). To verify its feasibility and the effect of the proposed optimal gait pattern from the point view of the integrated system (human and exoskeleton), simulations were performed in the cases of walking on level ground and stair ascent/descent. Experiments such as on the metabolic cost of the human body with or without the assistance of the exoskeleton were conducted, and the power consumption of the exoskeleton was assessed, with the aim of improving the efficiency of the integrated system.

## I. INTRODUCTION

Trials for minimizing energy consumption and enhancing energy efficiency have been timely issues in the engineering. But, there have been few studies on the powered robotic exoskeletons or legged type robots for lower-limb muscle power assistance, particularly concerning their efficiency, which is frequently researched on in relation to wheeled-type vehicles. The exoskeletons adapted by the lower limbs are currently too underdeveloped to enhance the performance of the human locomotors in the military and industry, and to be effectively used by elderly people with mobility impairments [1]. The proposed concepts concerning the improvement of the system efficiency and the activation of a system with low electricity consumption are among the timely robotic challenges with regard to humans' surroundings. Even when compared with orthotics, which provide powered assistance in daily lives or industries, exoskeletons can adjust to varying gait dynamics much better than a passively and rigidly assistive method can. Further, if the exoskeletons are not oriented by continuous passive motion for rehabilitation, which means that they do not need

Manuscript received July 16, 2010. This work was supported by the MKE(Ministry of Knowledge Economy), Korea, under the C7000-1011-0002 support program supervised by the NIPA(National IT Industry Promotion Agency) NIPA-2010-C7000-1011-0002, and a grant from Construction Technology Innovation Program(CTIP) funded by Ministry of Land, Transportation and Maritime Affairs (MLTM)

S. Lee is with the Department of Mechanical Engineering, Hanyang University, Seoul, Korea (phone: +82-31-400-4062; fax: +82-31-406-6398; e-mail: hopezic@gmail.com).

W. Kim. is with the Department of Mechanical Engineering, Hanyang University, Seoul, Korea (e-mail: mechawans@gmail.com).

M. Kang. is with the Department of Mechatronics Engineering, Hanyang University, Seoul, Korea (e-mail: wowmecha@gmail.com).

J. Han is with the Department of Mechanical Systems Engineering, Hansung University, Seoul, Korea (e-mail: jshanjs@gmail.com)

C. Han is with the Department of Mechanical Engineering, Hanyang University, Gyeonggi-do, Korea (e-mail: cshan@hanyang.ac.kr).

to adapt a firmly attached method, the reduced degrees of freedom in the system will make a person feel uncomfortable when she/he adapts or wears the exoskeleton [2-3]. In a study that was conducted on partially attached types of exoskeletons, the "operator" was defined as the wearer or pilot of the exoskeleton. In this case, the exoskeleton is driven and assisted by the pilot's allowable joint limit boundary. This certifies that the exoskeleton and the wearer include the construct of riding onto the system [4]. The wearer/pilot of the exoskeleton should be comfortable when riding the exoskeleton or taking it in, that's why the partial attachment method is more reasonable than the one presented in the previous relevant researches. This kind of human-robot integrated system presupposes that the stability of the robotic locomotors is guaranteed, that the use of the wearer/pilot's muscle power does not exceedingly increase the bounded constraints, and that the dynamic performance can be upgraded by minimizing the energy consumption of the proposed system.

Therefore, this study aimed to derive the feasible swing trajectory that would make the energy consumption of the joint torques for the exoskeleton the least possible one not only for the level-ground gait pattern but also for stair ascent/descent ambulation. The proper swing trajectories of the lower limb were fundamentally based on the function distributions and on the dynamic manipulability ellipsoid (DME) theory, which measures and mathematically quantifies the characteristics and dynamic performance of the exoskeleton. The model structure and the values of the model parameters were determined using the gait data collected from the young and healthy male subjects, and it was regarded that it is the combination of the mechanical. To verify the feasibility and effect of the redefined swing trajectory, simulations and experiments were conducted under conditions like walking on level ground and ascending/descending a staircase. During the experiments, the wearer's metabolic costs and the energy consumption of the powered robotic system were assessed, with the goal of improving the efficiency of the human-robot integrated system.

## II. DEFINITION OF THE TARGET TASK

### A. Analysis of Gait and Posture

Human locomotion is divided by phase during the whole sequence of walking, and by posture at each division. The whole sequence of gaits for the young and healthy subjects can be separated by stance and swing phase. The swing phase when a given foot is in the air almost entirely depends on the effect of gravity. Therefore, in this paper, the generated

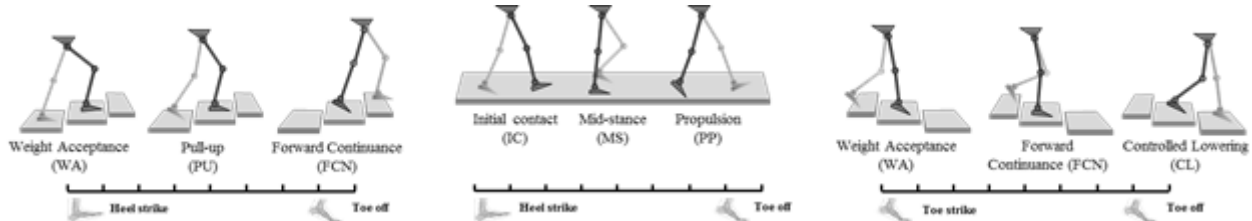


Fig. 1. Human-gait cycle analysis based on leg function distribution in the cases of level-ground walking and stair ascent and descent ambulation.

optimal gait pattern in the stance phase is discussed in light of the minimization of the energy consumption of the human-robot integrated system, except for the swing phase cases (Fig. 1).

The locomotion on a level ground, under normal walking conditions, is simply distributed in the following stages: initial-contact (IC) period - heel strike to forefoot loading; midstance period (MS) - forefoot loading to heel strike; and weight propulsion (WP) period - heel raise to toe-off. From another point of view, stair ambulation (ascent/descent) has more details with regard to the normal walking conditions.

The stance phase of stair ascent is partitioned into three sequences: weight acceptance (WA), pull-up (PU), and forward continuance (FCN). In the case of walking down the stairs, the stance phase is transformed into three subphases: WA, FCN, and controlled lowering (CL). Especially, the patterns for normal stair climbing show the dominant role of the knee during WA and PU, with supporting roles played by the hip and ankle. During FCN, the ankle plays the major role, with relatively little contribution from the knee and hip [5-8]. Similarly, the divisions for the ascent and descent phases were modified onto a 2D space, specifically on the sagittal plane, because 74% of the work done at the hip, 85% at the knee, and 93% at the ankle proceed in the sagittal plane during a single gait cycle [9-10].

As the vast majority of gait work is done in the sagittal plane, the ability to move in the coronal and transverse planes during human gaits would be overshadowed by the sagittal-plane function. Even though the gaits were categorized into three to five different stages in the past studies and the lower limb primarily functions not only to support and balance the body weight but also to raise the body weight onto the supporting stage, human walking can be divided into two dominant steps—IC and WP, or the toe-off and toe/heel strike stages—considering the goal of the system and the target subjects (Fig. 2).

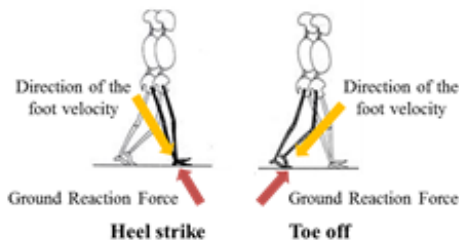


Fig. 2. Function stage distribution at the stance phase.

### B. Definition of the Target Task

Due to of the excessive driving torques in the stance phase, the exoskeleton system runs through cost-plenty energy at the IC and WP stages. The proposed gait pattern generation algorithm breaks through this limitation by focusing on deriving the proper joint angles. In this study, two different energy-efficient gait patterns are proposed based on the DME theory: walking on level ground and stair ascent/descent ambulation. These patterns, which aim at minimizing the energy consumption of the exoskeleton system, were simulated through the generation of a feasible trajectory during a gait cycle.

The GRF vector passes through the hip joint, eliminating the need for hip extensor activity, and the direction can be towards prolongation between the contact point from the toe/heel and the hip [11]. Supposing that the vectors made by the final contact point's velocity and the GRF are on the same line of prolongation, the exoskeleton consumes less energy than the vectors that do not align with the line (Fig. 2). The aforementioned estimated energy-efficient patterns were assessed through the experiments that were conducted to compare the human metabolic costs, such as oxygen consumption and CO<sub>2</sub> emission, and to measure the exoskeleton's power consumption, such as its current value during locomotion, specifically during IC and WP (Fig. 3). Through the conventional protocol of the biomechanics, the experiments where the metabolic costs for the human body were performed for 30 min. In the case of stair ascent/descent ambulation, however, as there were no stairs that could be climbed up and down for 30 min, and as at that moment the exoskeleton is not independent of the power line, and there wear no step which is allowable for walks during 30min. The experiments focused only on walking on level ground.

## III. OPTIMAL GAIT PATTERN GENERATION ALGORITHM

### A. Function Distribution in Stance Phase

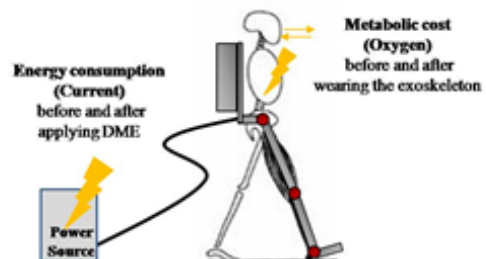


Fig. 3. Strategy for feasibility verification.

There have been unclear definition of stair ascent, and with regard to the results of the experiments that were conducted on healthy young subjects in this study, the trajectories that were made in terms of toe strike were in accordance with the same at heel strike. The angle distributions from  $\pm 2$  to  $\pm 5$  degrees varied at the moment of initial contact, and the deviations in the hip joint were slightly different from those in the other joints. This is because the width and height of the staircase affected the subjects, and they determined their own gait patterns and naturally controlled the joint angles as far as they could ascertain these.

In this study, the two dominant functions under the level-ground walking condition were decided: heel strike (supporting and balancing the body weight) and toe-off (propelling and raising the body). When it comes to stair ascent ambulation and walking on level ground, the underlying strategy is that the heel strike and toe-off functions are ordinarily adopted. When the pilot intends to support and balance the body weight, heel strike plays a part in the support function. When the pilot, on the other hand, intends to propel the body, toe-off undertakes the propulsion function (Table 1). The cases of level-ground walking and stair ascent/descent were set for adaptation by the same pattern generation algorithm.

### B. Concept of Dynamic Manipulability Ellipsoid

Manipulability ellipsoids provide an approximate description of the maximum available performance, such as the ability to perform velocities and accelerations at the end effector or to exert forces on the environment of a manipulator in a given posture. This is an advantageous way of designing the operational phase, determining the feasible structure of the manipulator, and finding the best configuration to execute a given task. The incremental kinematics of a manipulator is modeled by the pertinent equations.

This report uses the generalized inertia ellipsoid, and the change in kinetic energy can be expressed as in (1).

$$\Delta KE = -\frac{1}{2} \Delta \dot{\mathbf{u}}^T \mathbf{D} \dot{\mathbf{u}} \quad (1)$$

$\Delta \dot{\mathbf{u}}$  is the change in the foot velocity, which is equivalent to the foot velocity with respect to the ground immediately prior to the impact. A quadratic surface associated with (1) can be defined as

$$\mathbf{u}^T \bar{\mathbf{J}}^T \mathbf{D} \bar{\mathbf{J}} \mathbf{u} \leq 1 \quad (2)$$

This equation is the dynamically consistent generalized

TABLE I  
FUNCTION DISTRIBUTION UNDER LEVEL-GROUND WALKING  
AND STAIR AMBULATION CONDITION

Level-ground walking	Stair ambulation (ascent)	Stair ambulation (descent)
Heel strike	Heel/toe strike (not clearly defined) $\rightarrow$ heel strike	Toe strike
Toe-off	Toe-off	Toe-off

TABLE II  
UNITS FOR THE DME PARAMETER

Symbol	Quantity
$l_i, l_{ic}$	link variables (i-th link length, length from the center of the mass to the i-th joint)
$\theta$	joint variables (joint angle vectors)
$\tau$	joint torque vectors
$M(\Theta)$	$n \times n$ positive definite diagonal inertia matrices
$V(\Theta, \dot{\Theta})$	Coriolis, centrifugal force matrices
$G(\Theta)$	gravity matrices

inverse of the Jacobian matrix shown in (2) instead of the simple inverse.  $\bar{\mathbf{J}}^T \mathbf{D} \bar{\mathbf{J}}$  is called the ‘‘pseudo kinetic energy matrix.’’ This equation can be applied to the kinematics of the proposed system. For a fixed configuration of the leg relative to the point mass, the non-zero element of the joint velocity vector consists only of the forward velocity of the point mass and its vertical velocity, which can be related to the walking height. For a given change in the end effector velocity, the loss of kinetic energy will be maximum if the direction of the velocity is along the minor axis of the DME; likewise, the energy loss will be minimum if the direction of the velocity change coincides with the major axis (Fig. 4) [12-13].

### C. DME Analysis

The angle at the ankle joint is not important in the human locomotion at the moment that the heel strikes the ground, but it has a significant role at the toe-off stage. Therefore, the exoskeleton can be regarded as a 2DOF manipulator at the heel strike stage and is considered a 3DOF manipulator at the toe-off stage. Similarly, the exoskeleton can be equated with a 3DOF manipulator during stepping on a staircase, which consists of the heel strike and toe-off stages (Fig. 2).

The state space equations of the exoskeleton are represented by the following equations. As indicated prior to this part, DME is the main parameter that represents the angular velocity in relation to each joint and the line velocity of the links on the sagittal plane traced by the end effector: the toe or the heel of the leg. As DME describes the posture and velocity of the platform, a dynamic analysis of its study (i.e., numerical investigations of the behavior of the exoskeleton) should be done (Table 2).

$$\tau = M(\Theta) \ddot{\Theta} + V(\Theta, \dot{\Theta}) + G(\Theta) \quad (3)$$

$$\Theta = \begin{bmatrix} \theta_1(t) \\ \vdots \\ \theta_n(t) \end{bmatrix}, \quad \tau = \begin{bmatrix} \tau_1(t) \\ \vdots \\ \tau_n(t) \end{bmatrix}$$

The end effector and joint velocities are shown in (4).

$$\mathbf{v} = \mathbf{J}(\Theta) \dot{\Theta} \quad (4)$$

From normalized joint angular acceleration and joint torque, partially differentiated equations of joint velocity are represented as in (5) and (6) below.

$$\dot{\hat{v}} = \hat{J}M^{-1}(\Theta)\hat{\tau} \quad (5)$$

$$\hat{\tau} = \hat{M}(\Theta)\hat{J}^{-1}\dot{\hat{v}} \quad (6)$$

in which,

$$\hat{J} = T_a J \quad (7)$$

$$\hat{M}(\Theta) = T_r M(\Theta) \quad (8)$$

$$T_a = \text{diag} \left[ \frac{1}{\tilde{v}_{1\max}}, \frac{1}{\tilde{v}_{2\max}}, \dots, \frac{1}{\tilde{v}_{m\max}} \right] \quad (9)$$

$$T_r = \text{diag} \left[ \frac{1}{\tilde{\tau}_{1\max}}, \frac{1}{\tilde{\tau}_{2\max}}, \dots, \frac{1}{\tilde{\tau}_{m\max}} \right] \quad (10)$$

Hence, DME is simply formulated as in (11) [6].

$$\hat{\tau}^T \hat{\tau} = 1 \quad (11)$$

#### D. Simulation based on DME

As shown by the attack angle, energy consumption can be generally expressed by a change in kinetic energy. If the direction of the velocity is along the minor axis of the DME, as shown in the first figure, the energy loss will be maximized. In this study, the second concept (fitting the direction of the velocity change to the major axis of the DME) was applied to the locomotion of the exoskeleton (Fig.4). The state equation was calculated, and the DME parameter was simulated on MATLAB (Fig. 5). The walking parameters of the support and propulsion functions were completed. The DME of the 2DOF manipulator, which is made up of the hip and knee

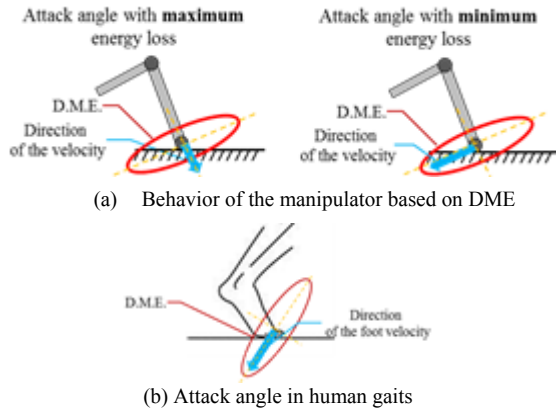


Fig. 4. Attack angle based on DME analysis

TABLE III  
LINK PARAMETER OF THE EXOSKELETON

Issue	Unit	Quantity
Length 0 ( $l_0$ )		0.4
Length 1 ( $l_1$ )	m	0.4
Length 2 ( $l_2$ )		0.29
m1		3.26
m2	kg	3.26
m3		4.2
Weight	kg	20

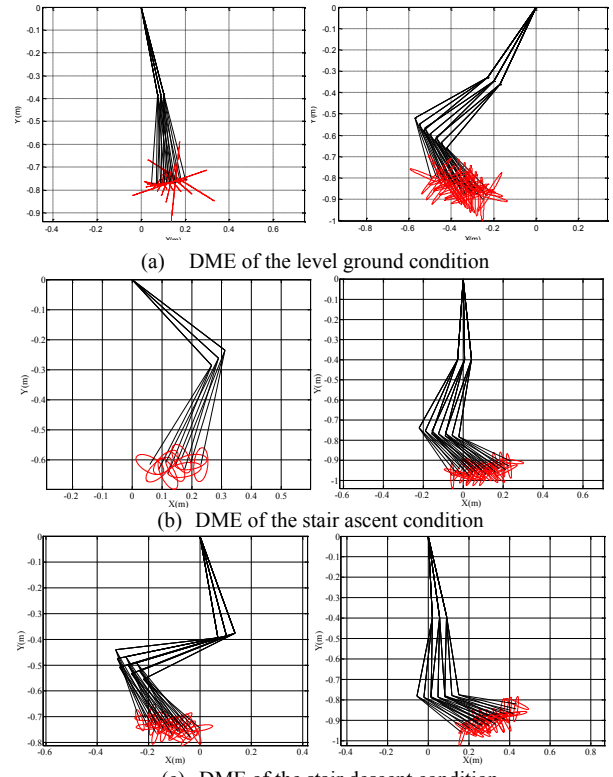


Fig. 5. DME of the various ground conditions

joint, was computed for the heel strike stage. Likewise, the DME of the 3DOF manipulator, which was made up of the hip, knee, and ankle joint, was computed for the toe-off stage. In the robot's dynamic modeling, every link parameters e.g. link length and weight of each segment are applied to the standard of young and healthy subjects. Likely, joint parameters related with hip, knee and ankle are theta 1, 2 and 3 in the schematic model of the exoskeleton (Table 3).

A simulation of energy-efficient gait pattern generation was performed with  $\pm 10$  degree range as following angle distributions of the standard subject. And it was worked by 1 degree level due to resolution of the actuator implemented in the exoskeleton. Each function – support and propulsion throughout the stance phase features heel/ toe strike and toe off stages; the optimum solutions are deduced by the alignment between direction of GRF and major axis of DME. The simulation results are come from the division of walking conditions and stages (Table 4). This result assumes an aspect of general human gait pattern, in specific, walking on level

TABLE IV  
SIMULATION RESULT OF OPTIMAL GAIT PATTERN GENERATION  
BASED ON DME

	Level-ground		Stair ascent		Stair descent	
	HS	TO	HS	TO	TS	TO
Hip joint	15°	-35°	32°	-4°	8°	10°
Knee joint	-9°	-20°	-70°	-25°	-9°	-87°
Ankle joint	-	-15°	-	-16°	-23°	16°

Heel strike = HS, Toe off = TO, Toe strike = TS

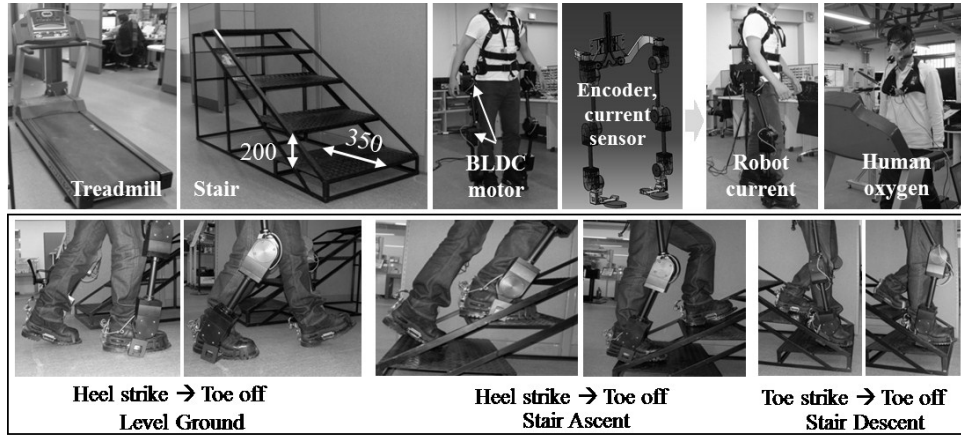


Fig. 6. Method and setup for the experiments

ground, theta 1, 2 and 3 come out 15 deg., -9 deg., null for heel strike stage; -35 deg., -20 deg., -15 deg. for toe off stage respectively. Difference between statistical datum and simulation results lies in the range of 3 to 5 degree. This is because human has evolved over a long period of time to pursue an objective of minimizing energy consumption.

#### IV. EXPERIMENT

##### A. Method: Population and Protocol and Set-up

The dynamic gait data acquired from the healthy young subjects (age:  $24 \pm 3$  years; stature:  $1.8 \pm 0.05$  m; body weight:  $78 \pm 5$  kg) were used to provide powered robotic exoskeleton system inputs and outputs during the stance phase of a walking gait, and system identification techniques were applied to the data to find the parameter values for a kinematic system model. Left and right lower-limb data were collected for several trials at each speed.

The informed consent of each subject was obtained after the full explanation of the tests. Before the experiments, the subjects were made to undergo a 10-min habituation period, which involved walking with the exoskeleton on level ground and for a few steps, and before the resist-and-assist condition, they were made to undergo an additional 5-min habituation period under the specified conditions. The staircase that was used was designed and custom-built specifically for this study. It consisted of four independent steps, and the step dimensions (height: 200 mm; tread: 350 mm) complied with the building regulations for common-use stairs. The gait cycle for stair ascent was defined by heel strike, as in the level-ground walking on the first step, through the toe strike of the same foot on the third step.

Statistical analyses were accomplished using MetaMax™ 3B. The experiment is carried out with assist of exoskeleton and without assist during 30 min. The experiments without assist of exoskeleton condition are separated into 2 parts – without load and with 40kg load. Herein, collected  $\dot{V}O_2$  (ml/min) data were scaled to both body mass ( $\dot{V}O_2$ -BM), by dividing  $\dot{V}O_2$  by the individual's body mass (kg), and to total mass ( $\dot{V}O_2$ -TM), by dividing  $\dot{V}O_2$  by body mass plus total

added mass (all equipment, measuring device - approx. 3kg, plus mass of exoskeleton)[14].

##### B. Result

Applying the results of the previous simulations, which include the optimal joint angle distributions based on DME analysis, to the proposed system, the experiments were performed at different walking conditions (Fig. 6). The sum of the current at every joint when the system was driven on the fairway and stairway was determined. Fig. 7 shows the current before the adaptation of the DME process, and the next figure shows the results after the adaptation of the process. This allows the comparison of the mean values of the currents before and after the application of the DME. Accordingly, due to the DME process, the proposed system was found to have consumed currents as low as 10% of the minimized one in the case of level-ground walking, 5% at stair ascent, and 10% at stair descent.

As seen in the result,  $\dot{V}O_2$  yielded statistically significant increase with 40kg load, it costs the maximum value - 992ml/min (Table 5). Energy consumption of human body has top ranked at this moment and vice versa, it is lower than that is done by the assistance of exoskeleton. However, under the normal walking condition, an operator with exoskeleton uses up more oxygen than the operator without the exoskeleton, the experiment has following result – 667ml/min (with exoskeleton) and 595ml/min (without exoskeleton). Mean  $\dot{V}O_2$ -TM with exoskeleton gets the minimum metabolic cost as 6.47ml/min/Kg, it assures that oxygen consumption rate (per unit mass) is on the lowest cost

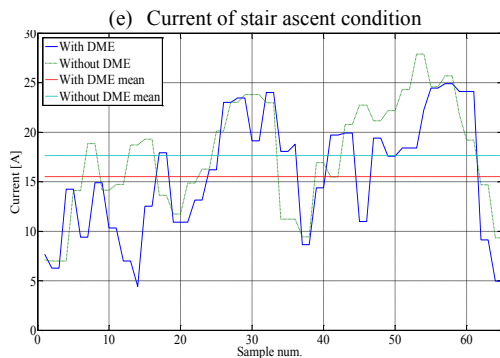
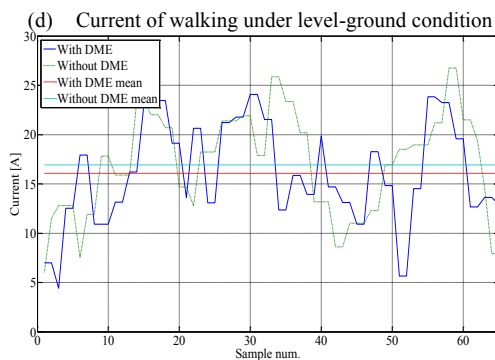
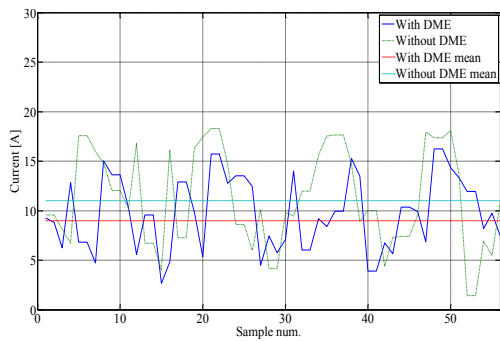
TABLE V  
RESULT ABOUT METABOLIC COST OF EACH DEVICE CONDITION AND LOAD

	EXO	No-EXO	
	EXO-20Kg	Load-0Kg	Load-40Kg
$\dot{V}O_2$ [ml/min]	667	595	992
$\dot{V}O_2$ -BM [ml/min/Kg]	8.33	7.43	12.4
$\dot{V}O_2$ -TM [ml/min/Kg]	6.47	7.16	8.06
$\dot{V}CO_2$ [ml/min]	803	352	1037

EXO = With exoskeleton, No-EXO = Without exoskeleton

when using the exoskeleton. Therefore, human with exoskeleton runs through approximately 10% less energy than without the exoskeleton under walking on level-ground condition – from 7.16ml/min/Kg to 6.47ml/min/Kg. The DME simulation results are applied to the experiments, mean current value has a tendency to be minimized around 5 to 10%, the energy consumption of the exoskeleton system is decreased by adapting the proposed algorithm i.e. 5% decrease for stair ascent condition; 10% drop-off under level-ground walking and stair descent condition.

Therefore, human body consumes 10% less energy and the exoskeleton uses up 5 to 10% minimized energy by employing the proposed gait pattern generation algorithm throughout the experiment. The above-described trials for minimizing energy consumption through DME analysis can enhance energy efficiency with respect to the exoskeleton adapted by the lower limb, and the success in overcoming the aforementioned robotic challenges will obviously have a positive effect on improving humans' surroundings.



(f) Current of stair descent condition

Fig. 7. Energy consumption of the exoskeleton

## V. CONCLUSION

This study proposed energy-efficient gait pattern and its trajectory of the exoskeleton through the simulation based on DME theory at two different functions distribution. And this pattern is employed to the experiment for feasibility verification. The experimental results are compared with wearing the exoskeleton and not wearing it. Mean value of current was checked for the exoskeleton system and metabolic cost for human body. Accordingly, the experiment results from human body and the exoskeleton, and DME theory based on function distributions is feasible for the energy-efficient gait pattern generation. It is possible for the exoskeleton to lose its weight by use of improving efficiency of the exoskeleton. Supposed that the weight of battery pack is fixed by the operation time, total mass can be reduced and as well as the efficiency can be enhanced. For going future study, more articulations, e.g. tiptoe would be considered.

## REFERENCES

- [1] G Okamura J., Tanaka H., Sankai Y., "EMG-based Prototype-powered Assistive System for Walking Aids", Proceedings of the Asian Symposium on Industrial Automation and Robotics (ASIAR'99), Thailand, pp. 229-234, 1999.
- [2] Kao, P., Ferris, D. P., "Motor Adaptation during Dorsiflexion-assisted Walking with a Powered Orthosis", *Gait & Posture*, Vol. 29, Issue 2, pp. 230-236, 2009.
- [3] Hidler, J., Wisman, W., Neckel, N., "Kinematic Trajectories while Walking within the Lokomat Robotic Gait-orthosis", *Clinical Biomechanics*, Vol. 23, Issue 10, pp. 1251-1259, 2008.
- [4] Kazerooni H., Chu A., Zoss A., "On the Biomimetic Design of the Berkeley Lower Extremity Exoskeleton (BLEEX)", *Robotic and Automation, ICRA2005*, Proceeding of the 2005 IEEE International Conference, pp. 4345-4352, 2005.
- [5] Lee S., Yu S., Lee H., Hong S., Han C., Han J., "Proposal for a Modular-type Knee-Assistive Wearable Unit and Verification of its Feasibility", *The International Symposium on Automation and Construction*, Vol. 1, pp.187-194, 2008.
- [6] Kim W., Lee S., Yu S., Han J., Han C., "Gait Pattern Generation Algorithm Based on Dynamic Manipulability Ellipsoid for Lower Extremity Exoskeleton", *Japan-Korea International Joint Symposium on Dynamics and Control*, pp.233-235, 2009.
- [7] McFadyen B., Winter D., "An Integrated Biomechanical Analysis of Normal Stair Ascent and Descent", *Journal of biomechanics*, Vol. 21, pp. 733-44, 1988.
- [8] Duncan J., Kowalk D., Vaughan C., "Six Degree of Freedom Joint Power in Stair Climbing", *Gait Posture*, Vol. 5, pp. 204-10, 1997.
- [9] Eng, J., Winter, D., "Kinematic Analysis of the Lower Limbs during Walking: What Information can be Gained from a Three-dimensional Model", *Journal of Biomechanics*, Vol. 28(6), pp. 753-758, 1995.
- [10] Palmer, M., "Sagittal Plane Characterization of Normal Human Ankle Function Across a Range of Walking Gait Speeds", Master thesis, Massachusetts Institute of Technology, Cambridge, 2002.
- [11] Michael W., "Gait Analysis an Introduction", Oxford Orthopaedic Engineering Center, ELSEVIER, 2007.
- [12] Pasquale C., Mariano C., "The Dynamic Manipulability Ellipsoid for Redundant Manipulators", *ICRA1998*, Belgium May, pp.95-100, 1998.
- [13] James P., "The Mechanics of and the Robotic Design for Quadrupedal Galloping", the Ohio State University, 2001.
- [14] Gregorczyk KN, Obusek JP, Hasselquist L, Schiffman JM, Bensek CK, Gutekunst D, Frykman P, "The Effects of a Lower Body Exoskeleton Load Carriage Assistive Device on Oxygen Consumption and Kinematics during Walking with Loads", 25th Army Science Conference. 2006; Orlando, FL, USA, Nov. 27-30
- [15] Jim R., "Biomechanics in Clinic and Research: An Interactive teaching and Learning Course", Department of Allied Health Professions , ELSEVIER, 2008.